Nonlinear Dyn (2017) 87:459–474
DOI 10.1007/s11071-016-3053-1

ORIGINAL PAPER

A model establishment and numerical simulation of dynamic coupled hydraulic–mechanical–electric–structural system for hydropower station

Qianqian Wu · Leike Zhang · Zhenyue Ma

Received: 9 April 2016 / Accepted: 30 August 2016 / Published online: 8 September 2016

Abstract A nonlinear dynamic coupled model for hydropower station system, which contains the model of water-carriage system, water turbine system, speed governor system, generator's electromagnetic system, grid, shaft system of hydroelectric generating set, as well as the powerhouse, is established in this paper. Firstly, the simultaneous differential equations for coupled hydraulic–mechanical–electric transient process are set up based upon the theories of hydraulics, electrical machinery, etc., while the coupled structural models for shaft system of unit and powerhouse are built by means of finite element method. Secondly, a new method for investigating nonlinear dynamic properties of structures influenced by coupled hydraulic–mechanical–electric factors in different conditions is introduced with the help of user-programmable features from Ansys software. Finally, in order to verify the rationality, several numerical calculation methods are used to study the starting-up process of hydropower station. The results indicate that the model presented in this paper is adoptable for simulating specified condition and reflect the nonlinear dynamic characteristics of hydropower station comprehensively. In addition, the model can also be used to assess the operation safety and predict the structures reliability of hydropower station system, so as to provide some profitable reference for dynamic regulation during limited and transient conditions for hydropower station.

Keywords Hydropower station system · Coupled hydraulic–mechanical–electric model · Dynamic characteristics analysis

Q. Wu · Z. Ma
School of Hydraulic Engineering, Faculty of Infrastructure Engineering, Dalian University of Technology, Dalian 116024, Liaoning Province, China

L. Zhang (✉)
College of Water Resources Science and Engineering, Taiyuan University of Technology, Taiyuan 030024, Shanxi Province, China
e-mail: lkzhang@hotmail.com

Nomenclature

A	Area of penstock
a	Water hammer wave velocity
b_p	Permanent droop
b_t	Temporary droop
c_b	Clearance of bearing
c_{ij}	Damping cofficients, $i = x, y$; $j = x, y$
c_r	Air gap length of rotor
D	The cross section diameter of penstock
D_1	The diameter of water turbine
E'	Transient electromotive force (EMF)
e_b	Eccentricity of shaft axis
e_r	Eccentricity of rotor center
E_{fd}	Imaginary open-circuit EMF generated by field voltage
E_q	No-load terminal EMF

E'_q	Transient EMF of q-axis
f_e, f_m	Electric and mechanical frequency
f_{es}, f_{ms}	Electric and mechanical synchronous frequency
h	Thickness of oil film
H_i	Head in penstock at the node i
H_n	Net water head of water turbine
I, I_d, I_q	Stator current and corresponding d- and q-component
I_f	Excitation current
J	Moment inertia of the hydroelectric generating set
k_{ij}	Stiffness coefficients, $i = x, y$; $j = x, y$
K_P, K_I, K_D	Proportional, integral and differential gain of governor
L_p	Height of pad
L_r	Length of rotor
M_e	Electric torque
M_t	Mechanical torque
n	Mechanical speed of water turbine
n_s	Mechanical synchronous speed of water turbine
n'_1	Unit mechanical speed of water turbine
p	Oil pressure
P_e	Electric power (active output)
P_t	Power of water turbine
P'_1	Unit power of water turbine
Q'_1	Unit discharge of water turbine
Q_i	Discharge in penstock at the node i
R_a	Radius of shaft
R_b	Radius of journal
R_e	Resistance of transmission line
R_i	Inner radius of pad
R_L	Resistance of system load
R_o	Outer radius of pad
R_r	Radius of rotor
T_d	Reset time or dashpot constant
T'_{d0}	Open-circuit transient time constant of d-axis
T_e	Time constant of excitation
T_m	Water turbine inertia time constant
T_n	Accelerating time constant
T_w	Water inertia time constant
T_y	Servomotor response time constant
U_f	Excitation voltage
U_L	Load voltage of system
U_G, U_{Gd}, U_{Gq}	Stator terminal voltage and corresponding d- and q-component
X_e	Reactance of transmission line
X_L	Reactance of system load
X_d, X_q	Synchronous reactance of d-and q-component
X'_d	Transient reactance of d-component
y	Servomotor stroke of governor
α_p	Opening angle of pad
β	Angle between a point of support for pad and y-axis
Δy	Deviation value of water turbine servomotor stroke
δ	Power angle
δ_p	Swing angle of pad
η	Efficiency of water turbine
η_l	Angle between the calculation location and y-axis
θ_b	Deviation angle of bearing axis
θ_e, θ_m	Electric and mechanical rotation angle
λ	Dimensionless coordinate of pad along the shaft
τ	Guide vane opening
φ	Power factor
ψ	Inner power factor
ω_e, ω_m	Electric and mechanical speed
ω_{es}, ω_{ms}	Electric and mechanical synchronous speed

1 Introduction

In power system, the hydropower station is mainly responsible for power generation, pink load regulation, frequency regulation, and phase modulation, etc. The studies of station operation stability and structures vibration characteristics are very important to the corresponding systems. The operation of hydropower station is a complicated process which is interacted by several different subsystems. A complete model of the system is roughly comprised of the submodels including whole flow passage (penstock, volute and draft tube), water turbine, speed governor, generator, and structures (hydroelectric generating set and powerhouse), etc. The function of the coupled model is further required to simulate and analyze the hydraulic transient, the mechanical motion with speed regulation process, the electromagnetic transient and the structural vibration. On that

basis, the stability of the limited and transient conditions is able to be studied, and the vibration characteristics of mechanical and civil engineering structures can be investigated accordingly.

Generally, the research object in the whole flow passage mainly refers to the hydraulic transient process. The fundamental equations for one-dimensional (1D) water hammer were derived by Chaudhry [1], Collatz [2], and Wylie [3]. These equations named as governing equations of 1D transient flow can be solved by method of characteristics (MOC) and finite difference method (FDM). After that, special attention was given to the parameters involved in the equations, such as water hammer wave speed [4,5] and wall shear stress [5,6,6–8]. Meanwhile, the solution methods [1,3,9] were also discussed literarily. With the consecutive progress of computer technology, the numerical model of 3-dimensional (3D) transient flow calculated by computational fluid dynamics (CFD) was developed. In order to study the pressure fluctuation in the draft tube, Ruprecht and Helmrich [10] proposed a method to couple the 1D MOC with 3D CFD, which showed great improvement for the efficiency and precision of the numerical simulation [11–13].

The operation of the water turbine is a highly nonlinear dynamics process affected by the parameters including head, discharge, speed and guide vane opening. Hovey et al. [14–16] established the linear model of water turbine under many hypotheses. Then, with taking into account nonlinear behaviors, such as the elastic penstock and compressible water, the model was developed and improved to be of nonlinear form by many researchers [17,18]. With regard to the nonlinear model, the synthetic characteristics curves of water turbine, which are a group of diagrams generalizing the highly nonlinear behaviors of full condition, were essential to describe the model. Until now, it is barely possible to derive the numerical model and mathematical equations for the curves because of its discreteness and nonlinear properties; thus, the fitting and interpolation methods are usually employed to solve the transient process of water turbine with the aid of synthetic characteristics curves at present.

For the purpose of regulating the rotating speed of water turbine, the model for speed governor was developed. Paynter [19], Hovey [16] and Leum [20] set up the general guidelines about how to select control parameters. The common regulation law of proportional–integral–differential (PID) strategy includes three terms, namely the control to treat the current control error (proportional control), past control error (integral control) and predicted future control error (differential control), which is useful to guarantee the stability, rapidity and accuracy of governor [21,22]. Based on that, a number of studies were carried out [23–26] to improve the PID control strategy or further develop the new regulation laws. While the great contributions to regulation system of water turbine have been done by Chen's group [27–29] in recent years, which provided useful and significant reference for the development of this field.

The study about generator includes both electromagnetic and electromechanical transient analysis; the former is often used to analyze the power system faults, while the latter is applied to discuss the power system stability. Kilgore [30] and Wright [31] were treated as the pioneer of modeling synchronous generators. Afterward, the Heffron–Phillips generator model was established in 1952 [32] and adopted to investigate the stability of the power system. While Demllo et. al [33–35] studied the stability of the single generator supplying an infinite bus system with the model of synchronous generators.

In addition to the above subsystems, the hydroelectric generating set and powerhouse playing the important roles are also involved in hydropower station system. The shaft model of unit is usually simplified as a rotor-bearing system in numerical simulation, and the rotor is often treated as single disk with lumped mass, while the core of the guide bearing model is how to describe the dynamic characteristics of oil film. In the early stage, the oil film characteristics were equated to eight parameters obtained by experiment in the linear model [36]. Later, the nonlinear model appeared, with types of short bearing model, long bearing model [37] and finite element model [38,39]. Generally speaking, the analytic solution was derived from short or long bearing model under reasonable assumptions [40,41], but only numerical solution can be acquired if finite element model was used [39]. Besides the work on bearing oil film [42–44], another important research content of rotor-bearing system is the nonlinear dynamic response of the rotators. Due to the reason that related studies were carried out earlier, abundant achievements have been acquired and analogous research technique tends to be mature [45–49]. However, for the discussions about rotor-bearing system in the models mentioned above, most boundary conditions of bearings

were treated as fixed constrains, which is obviously different from the elastic structures shown as piers or plants in actual. Undoubtedly, the interaction relationship between the unit and powerhouse cannot be reflected by traditional way. For the powerhouse possessing the properties of mass concrete and complex form, the finite element method (FEM) is an appropriate way to establish the model, and two research contents were mainly focused on this model: (1) structural optimization and load transfer path [50,51] and (2) natural vibration characteristics and dynamic response [52,53]. Nevertheless, it needs to be pointed out that the shaft system was seldom included in the whole model establishment in these studies, while the work on coupled dynamic characteristics between them was rarely reported [54,55].

According to the descriptions mentioned above, it can be seen that although many effective and efficient studies of traditional structural vibration for unit and powerhouse have been done, and the abundant analysis of coupled hydraulic–mechanical–electric transient process [56–58] has also been carried out over the past few decades; nonetheless, the interaction between the coupled structural vibration and coupled transient process was not considered. On one hand, the former researches on structural vibration were too isolated with neglect of the influence of actual operation conditions changed. On the other hand, the latter ones were mainly focused on the stability problems without considering the effect of coupled transient process on the structures. Therefore, it is no doubt that both of them are limited to some extent; the advantage is that the above analysis is very careful and thorough on specific research object, while the disadvantage is that there is no establishment of whole system model for the purpose of forming comprehensive analysis framework. Obviously, with the increase in installed capacity and development of hydropower station (especially for pumped storage power station), the trend of giant structures and frequent transient process for the station has become the necessity. Meanwhile, the stability of coupled hydraulic–mechanical–electric and vibration properties of structure, as well as the interaction between them will also be increasingly evident. Hence, the isolated and independent investigation focusing only on respective areas, without consideration about the mutual influence between each other, cannot meet the requirement of theoretical research and engineering practice.

In view of this, a comprehensive hydropower system model consisted of hydraulic, mechanical, electric and structural subsystems is established in this paper. The models of 1D penstock, nonlinear water turbine, PID governor, third-order synchronous generator, coupled structure of unit shaft system and powerhouse, as well as nonlinear guide bearing are all included in the system. A practical hydropower station is taken as a numerical example for the starting-up condition to test viability and effectiveness of the system model. The results indicate that, on one side, the model proposed in this paper can be used to study the stability of coupled hydraulic–mechanical–electric transient process for hydropower station in limited and transient conditions. On the other side, various dynamic loads related to the hydraulic, mechanical and electric parameters can be simulated and applied on this platform, analyzing the dynamic characteristics of coupled structure model under the influence of multiple factors. The operation properties of hydropower station can be explained and described well according to this model, with the purpose of providing reliable guarantee for stable operation and structural safety of the system.

2 Models

A complex and coupled nonlinear system for hydropower station is established, as shown in Fig. 1. In order to illustrate the mathematical model, the system is decoupled into 5 modules, which are presented and introduced in Sects. 2.1–2.5, respectively. The definitions of symbols in various models can be seen in nomenclature.

2.1 Penstock model

It needs to be pointed out that although a more comprehensive analysis and higher accuracy for fluid properties can be provided by 3D penstock model, these characteristics are not within the scope of the study in this model at present stage. Aiming at the need for solving the discharge and head along the penstock in this section, a 1D penstock model with simple calculation and enough accuracy is selected here. The 1D model of penstock [1] is used to solve the discharge (Q) and head (H) in the flow passage of hydropower station system. In Fig. 2, the pressure conduit on upstream of the plant is the connection between the water turbine

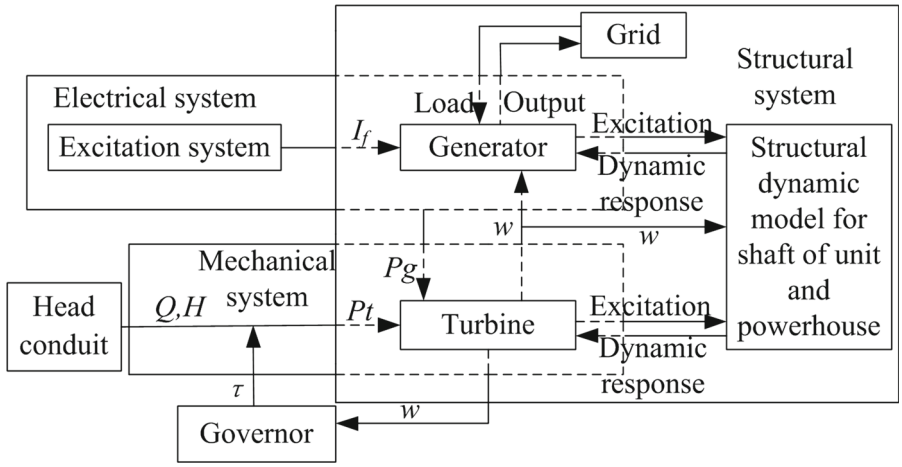

Fig. 1 Sketch of hydropower station system

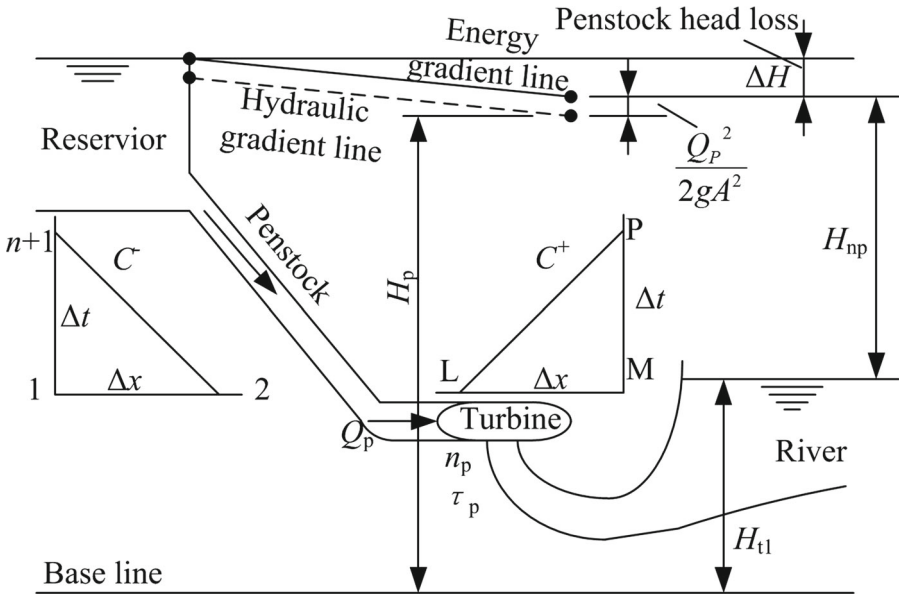

Fig. 2 Boundary conditions

and reservoir. The 1D transient flow in the penstock can be described as momentum equation and continuity equation

$$\frac{\partial Q}{\partial t}+\frac{Q}{A}\frac{\partial Q}{\partial x}+gA\frac{\partial H}{\partial x}+\frac{fQ|Q|}{2DA}=0 \tag{1}$$

$$\frac{\partial H}{\partial t}+\frac{Q}{A}\frac{\partial H}{\partial x}+\frac{a^2}{Ag}\frac{\partial Q}{\partial x}+\frac{Q}{A}\sin\alpha=0 \tag{2}$$

Taking use of Eq. (3) and Eq. (4) to mesh and discretize the above two equations

$$\begin{aligned}Q_i^{n+1}=&\frac{1}{2}(Q_{i+1}^n+Q_{i-1}^n)\\&-\frac{\Delta t Q_i^n}{2A\Delta x}(Q_{i+1}^n-Q_{i-1}^n)\\&-\frac{\Delta t g}{2\Delta x}(H_{i+1}^n-H_{i-1}^n)\\&-\frac{f}{8DA}(Q_{i+1}^n+Q_{i-1}^n)\left|(Q_{i+1}^n+Q_{i-1}^n)\right|\end{aligned} \tag{3}$$

$$\begin{aligned}H_i^{n+1}=&\frac{1}{2}(H_{i+1}^n+H_{i-1}^n)\\&-\frac{\Delta t Q_i^n}{2A\Delta x}(H_{i+1}^n-H_{i-1}^n)\\&-\frac{\Delta t}{2A\Delta x}\frac{a^2}{g}(Q_{i+1}^n-Q_{i-1}^n)\\&-\frac{\Delta t}{A}Q_i^n\sin\alpha\end{aligned} \tag{4}$$

where the subscripts i and n denote the position node i and time node n, respectively.

On this basis, the equations with $2i$ unknowns are composed of the corresponding boundary equations derived by MOC, as well as the above equations. The water turbine represents the downstream boundary condition of penstock whose positive characteristic equation at time step n is

$$Q_P = A\left(C_P - C_a H_P\right) \tag{5}$$

where

$$\begin{aligned} C_a &= g/a, \\ C_P &= \frac{Q_M}{A} - \frac{\Delta t}{A^2 \Delta x}\left(Q_M + A a_M\right)\left(Q_M - Q_L\right) \\ &\quad + C_a\left[H_M - \frac{\Delta t}{A \Delta x}\left(Q_M + A a_M\right)\left(H_M - H_L\right)\right] \\ &\quad + g\left(S_0 - S_f\right)\Delta t. \end{aligned}$$

Besides, the reservoir is treated as the upstream boundary condition for penstock, and the corresponding negative characteristic equation at time step n is given as

$$Q_1^{n+1} = A\left(C_N + C_a H_1^{n+1}\right) \tag{6}$$

where

$$\begin{aligned} C_N &= \frac{Q_1^n}{A} + \frac{\Delta t}{A^2 \Delta x}\left(Q_1^n - A a_1\right)\left(Q_2^n - Q_1^n\right) \\ &\quad - C_a\left[H_1^n - \frac{\Delta t}{A \Delta x}\left(Q_1^n - A a_1\right)\left(H_2^n - H_1^n\right)\right] \\ &\quad + \frac{\Delta t g Q_1^n}{A a_1}\sin\alpha - \frac{f \Delta t}{2DA^2} Q_1^n \left|Q_1^n\right|. \end{aligned}$$

in which, the subscripts 1 and 2 denote the two nodes of upstream boundary position, while M and L represent that of downstream boundary position at time n, respectively. P is the node at the end of downstream boundary at time $n+1$. If the boundary conditions of (H_1, Q_1) and (H_p, Q_p) are given, the velocity (discharge) and pressure (head) of all nodes in the penstock system can be obtained by simultaneous solution of Eqs. (3)–(6). H_1 means the water level of the reservoir, and Q_p is the operation discharge of water turbine.

2.2 Water turbine model

The water turbine converts the hydraulic power to mechanical power with the rotating equation written as

$$J\frac{\mathrm{d}\omega_m}{\mathrm{d}t} = J\frac{\mathrm{d}^2\theta_m}{\mathrm{d}t^2} = M_t - M_e \tag{7}$$

It can be seen that the operation status of water turbine is decided by the speed (ω), torque (M_t), discharge (Q) and opening (τ), while the comprehensive characteristic curves just plays the role of representing the nonlinear relationship among the four variables mentioned above, namely

$$\tau = f\left(n_1', Q_1'\right), \eta = g\left(n_1', Q_1'\right) \tag{8}$$

The water turbine models with characteristic curves were generally employed to study the transient process of turbine [59,60]. Due to the highly nonlinear characteristics of the curves, it is unable to establish a mathematical expression providing with clear physical meaning. In order to utilize the discrete data on the curves, it is needed to input these data into the computer, and then, the parameters of whole conditions can be obtained by fitting and interpolation methods. In this model, when the values of Q, n and τ for previous time steps are known, H_np and P_t (M_t) can be calculated by means of iteration method. As demonstrated in Fig. 2, the relationship between H_p and Q_p has the following expression as

$$H_p = H_{np} + H_{t1} - \frac{Q_p^2}{2gA^2} \tag{9}$$

The H_p and Q_p are acquired through simultaneous solution of Eqs. (9) and (5). The vane opening for this time step is calculated using the model of governor, while the value of speed can only be obtained after getting P_e (M_e) from the model of synchronous generator.

2.3 Governor model

The hydraulic governor provides a reliable rotating speed regulation for water turbine [61], as the load varies in power system. In this paper, a classical PID control strategy is applied in the model of governor. As shown in Fig. 3, the C_f is given as frequency command, and then, the transfer function from x to y can be expressed as

$$\begin{aligned} G(s) &= \frac{Y(s)}{X(s)} \\ &= \frac{K_D S^2 + K_P S + K_I}{b_p K_D S^2 + \left(b_p K_P + 1\right) S + b_p K_I} \\ &\quad \times \frac{1}{T_y S^2 + T_y S + 1} \end{aligned} \tag{10}$$

where x and y are the input (deviation ratio of rotating speed) and output (servomotor stroke) variables,

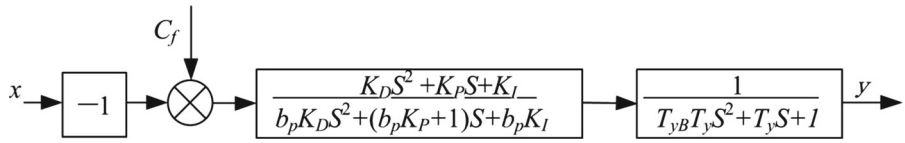

Fig. 3 Transfer function of the frequency regulation mode

respectively. Through the inverse Laplace transformation, a third-order differential equation is obtained

$$b_p K_D T_y y''' + \left(b_p K_P T_y + T_y + b_p K_D\right) y'' + \left(b_p K_I T_y + b_p K_P + 1\right) y' + b_p K_I y = K_D x'' + K_P x' + K_I x \tag{11}$$

According to the modern control theory, taking use of Eq. (11) to derive the state equation, a group of first-order differential equations can be acquired as [58]

$$\dot{x}_1 = x_2 + \beta_1 x, \dot{x}_2 = x_3 + \beta_2 x, \dot{x}_3 = -a_3 x_1 - a_2 x_2 - a_1 x_3 + \beta_1 x \tag{12}$$

where $\beta_0 = b_0, \beta_0 = b_1 - a_1\beta_0, \beta_2 = b_2 - a_1\beta_1 - a_2\beta_0, \beta_3 = b_3 - a_1\beta_2 - a_2\beta_1 - a_3\beta_0. a_1 = (b_p K_P T_y + T_y + b_p K_D)/b_p K_D T_y, a_2 = (b_p K_I T_y + b_p K_P + 1)/b_p K_D T_y, a_3 = b_p K_I/b_p K_D T_y. b_0 = 0, b_1 = K_D/b_p K_D T_y, b_2 = K_P/b_p K_D T_y, b_3 = K_I/b_p K_D T_y.$

The x_1 is solved by means of fourth-order Runge–Kutta algorithm in Eq. (12); then, the y is achieved through $y = x_1 + \beta x$. Finally, the vane opening can be obtained.

2.4 Synchronous generator model

For generator model, the subtransient can be ignored in general analysis of power system stability; thus, a third-order model of synchronous machine [32] is adopted to simulate the transient process of generator with appropriate accuracy and suitability, instead of the more complicated fifth-order model. The model of synchronous generator is used to describe the relationship of its internal electric parameters, in which the electric power (P_e), terminal voltage (U_G), and current (I) of the system can be obtained. Figure 4 is the phasor diagram of the salient-pole synchronous generator, and the relationship between the terminal voltage and stator current of the salient generator can expressed as

$$\begin{cases} U_{Gq} = E'_q - I_d X'_d \\ U_{Gd} = I_q X_q \\ U_G^2 = U_{Gq}^2 + U_{Gd}^2 \\ P_e = U_{Gq} I_q + U_{Gd} I_d \end{cases} \tag{13}$$

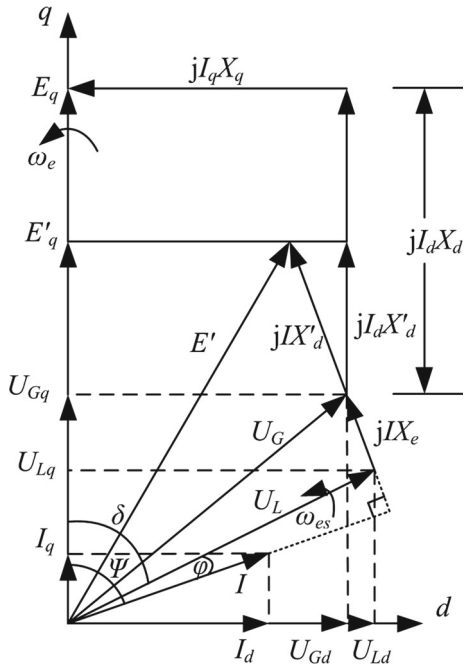

Fig. 4 Phasor diagram

The generator output is fed into the grid by transmission line supplying power consumption of the load. In order to consider the effect of grid, the characteristics that the load changes with the variation of grid voltage is adopted, using the constant impedance to represent load model. So, the relationship between terminal voltage and load voltage can be written as

$$\begin{cases} U_{Gd} = U_{Ld} + I_d R_e - I_q X_e \\ U_{Gq} = U_{Lq} + I_q R_e + I_d X_e \\ U_{Ld} = I_d R_L - I_q X_L \\ U_{Lq} = I_d X_L + I_q R_L \end{cases} \tag{14}$$

Taking use of the first formula in Eq. (13) and considering the relationship of parameters in Fig. 4, the connection between open-circuit terminal electromotive force (EMF) and transient EMF in q-axis can be obtained

$$E_q = E'_q + I_d(X_d - X'_d) \tag{15}$$

It should be pointed out that, since the subtransient process is not taken into account, the influence of

Fig. 5 Structural model

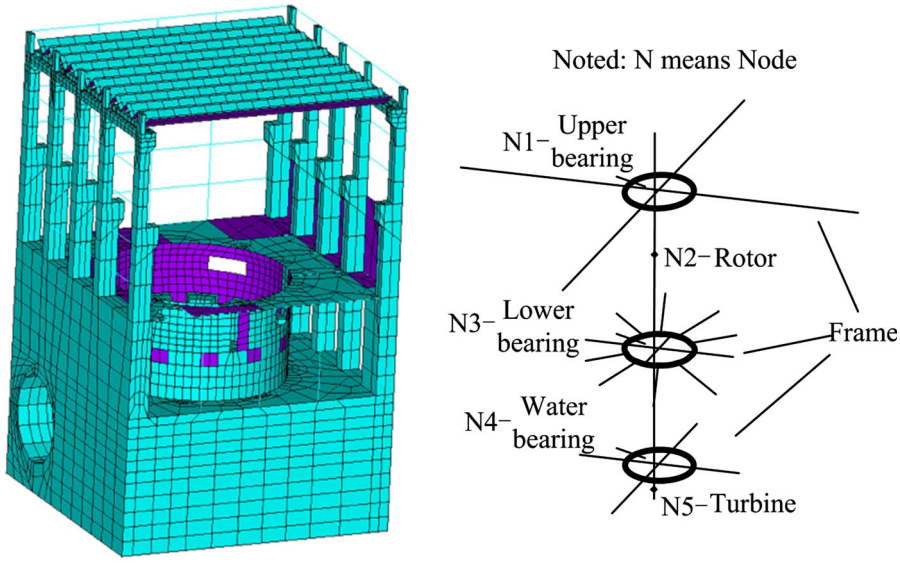

(a) Hydropower powerhouse model **(b)** Rotor-bearing model

damp winding of rotor and the resistances of stator are neglected accordingly during the derivation process. Moreover, due to the reason that the E'_{q} is not a constant, the differential equation of transient EMF can be derived with the help of both filed circuit equation and Eq. (15)

$$T'_{d0}\frac{\mathrm{d}E'_{\mathrm{q}}}{\mathrm{d}t} = E_{\mathrm{fd}} - E'_{\mathrm{q}} - I_{\mathrm{d}}(X_d - X'_{\mathrm{d}}) \tag{16}$$

Based on the regulation method with voltage deviation, the equation of auto-excitation system of generator has the expression as

$$T_{\mathrm{e}}\frac{\mathrm{d}\Delta E_{\mathrm{fd}}}{\mathrm{d}t} = -\Delta E_{\mathrm{fd}} - K_{\mathrm{v}}\Delta U_{\mathrm{G}} \tag{17}$$

According to $\omega_{\mathrm{e}} = p_n\omega_{\mathrm{m}}$ and $P = M\omega_{\mathrm{m}}$(p_n is the number of pole pairs), the mechanical speed and torque in the rotor motion equation can be converted into corresponding electric speed and power, and then, the motion equation of rotor can be expressed as the per unit form

$$T_{\mathrm{m}}\frac{\mathrm{d}\omega_e^*}{\mathrm{d}t} = \left(P_{\mathrm{t}}^* - P_{\mathrm{e}}^*\right)/\omega_{\mathrm{e}}^* \tag{18}$$

where $T_{\mathrm{m}} = J\omega_{\mathrm{ms}}^2/S_N$, S_N means the nominal capacity (basic value of power). And the unit rotating speed can be calculated by Eq. (18). The superscript * represents the per unit parameter.

2.5 The structure models

As shown in Fig. 5a, the typical structure of ground powerhouse includes the generator slab, fan cover, piers, volute, draft tube concrete. The bottom boundary constraints of powerhouse model are fixed, while the rest parts are free, and water pressure fluctuation under different conditions can be exerted on the structure, and the shaft system of hydraulic generating set is usually simplified as rotor-bearing system. As a reliable method to simulate complicate structures, FEM is adopted to establish the model in this paper. On the basis of design drawings for one actual powerhouse, a 3D structure simulation is carried out by the typical and widely used FEM software Ansys. In the powerhouse model, the elements solid45, solid90, shell63 and beam188 are used to simulate large concrete structures, slabs, fan cover and pillars, respectively, and the whole powerhouse model is depicted in Fig. 5a. For the shaft system model of unit, the moment of inertia of rotor and turbine as well as the gyroscopic moments are all neglected because the study in this paper is mainly focused on the radial dynamic response of rotating machinery. The elements of beam188, mass21, combine14 are used to simulate shaft, rotor, as well as turbine and guide bearing, respectively, and a typical model of shaft system is depicted in Fig. 5b. The dynamic characteristics parameters k_{ij} and c_{ij} in guide bearing represent the stiffness and damping of com-

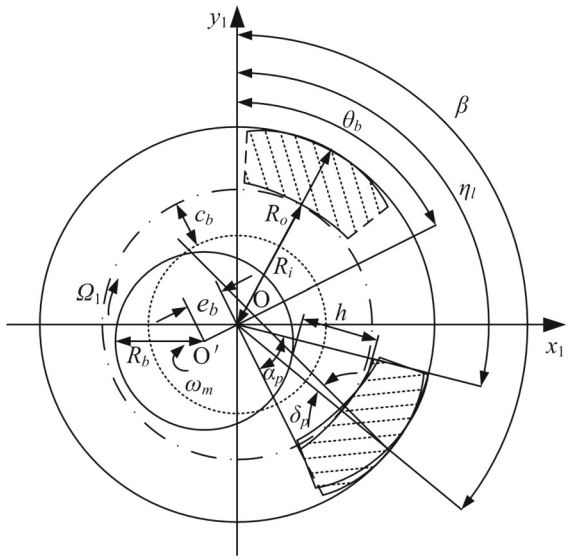

Fig. 6 Tilting pad guide bearing

bine14, respectively, and the shaft system model of unit is mounted on the powerhouse by constraint equations.

Figure 6 is the diagram of tilting pad guide bearing model. When the rotating speed of shaft is relatively slow, the Reynolds equation can be employed to describe the radial oil film pressure fields around pads in the guide bearing, namely

$$\frac{\partial}{\partial x_1}\left(\frac{h^3}{\mu}\frac{\partial p}{\partial x_1}\right)+\frac{\partial}{\partial y_1}\left(\frac{h^3}{\mu}\frac{\partial p}{\partial y_1}\right)=6U\frac{\partial h}{\partial x_1} \tag{19}$$

in which the parameters are referred to the nomenclature, and the non-dimensional form of corresponding equation is

$$\frac{\partial \bar{h}}{\partial \eta_l}\left(\bar{h}^3\frac{\partial \bar{p}}{\partial \eta_l}\right)+\gamma^2\left(\bar{h}^3\frac{\partial \bar{p}}{\partial \lambda}\right)=6\frac{\partial \bar{h}}{\partial \eta_l} \tag{20}$$

where $x_1 = R\eta_l, \lambda = y_{1/}(L_\mathrm{b}/2), \lambda \in [-1, +1]$, and the dimensionless thick parameters of the oil film have the expression as

$$\bar{h} = 1+\varepsilon\cos(\eta_l-\theta_p)-(1-c'/c_b)\cos(\beta-\eta_l) +\delta_p/b\sin(\beta-\eta_l) \tag{21}$$

in which $\varepsilon = e_\mathrm{b}/c_\mathrm{b}$ is eccentricity of the guide bearing and $b = c_\mathrm{b}/R_\mathrm{b}$ is the ratio of clearance and radius. Define u and v as circumferential and radial velocity of oil film, respectively; then, the dynamic Reynolds equation can be explicated as

$$\frac{\partial \bar{h}}{\partial \eta_l}\left(\bar{h}^3\frac{\partial \bar{p}}{\partial \eta_l}\right)+\gamma^2\left(\bar{h}^3\frac{\partial \bar{p}}{\partial \lambda}\right) =6\frac{\partial \bar{h}}{\partial \eta_l}+6(u\sin\eta_l+v\cos\eta_l) \tag{22}$$

Make the definition of $\Pi = \bar{h}^{1.5}\bar{p}$; then, Reynolds equation can be rewritten as

$$\frac{\partial^2\Pi}{\partial\eta^2}+\gamma^2\frac{\partial^2\Pi}{\partial\lambda^2}-a\Pi =\bar{h}^{-1.5}\left[6\frac{\partial\bar{h}}{\partial\eta}+6\,(u\sin\eta+v\cos\eta)\right] \tag{23}$$

where $a = \frac{3}{4}\left[\left(\frac{\partial\bar{h}}{\partial\eta_l}\right)/\bar{h}+\frac{2}{\bar{h}}\frac{\partial^2\bar{h}}{\partial^2\eta_l}\right]$

The oil pressure can be acquired from Eq. (23) by FEM; then, the oil film force can be generated through the integration of element solution [39]. The respective partial derivatives of the force with respect to the displacement and velocity in direction of x_1, y_1 are

$$k_{is} = \frac{\partial f_i}{\partial s}, c_{is} = \frac{\partial f_i}{\partial \dot{s}} \tag{24}$$

in which i and s represent x_1 and y_1, respectively. After solving the stiffness and damping coefficients for every pad, the corresponding coefficients for whole bearing can be obtained through combining all pads.

3 The hydropower station system

The type of turbine named as HL180-LJ-410 conforming to the Chinese naming code is selected as the object in this paper, and the corresponding meaning is a Francis turbine whose specific speed is 180 m KW, vertical arrangement, metallic volute, and the diameters of runner is 410 mm. The duration of starting-up process for numerical simulation is 43 s, and the process of voltage building-up for generator begins at $t = 27$ s when the rotating speed, output and discharge of water turbine are stable. Therefore, the generator is under no load during the starting-up process for unit, without referring to electromagnetic transient process. However, the excitation current produced from the process of voltage building-up is taken into account, which means that the mechanical eccentric force and unbalanced magnetic pull (UMP) [45] acting on the rotor system have to be considered. The loads generated due to the hydraulic–mechanical–electric factors are the connections between hydraulic–mechanical–electric subsystem and structure subsystem. The data of the penstock,

Table 1 Data of models

Nominal/no-load value of turbine						Length/diameter of penstock (m)		
Head (m)	Weight (t)	Turbine eccentricity (mm)	Discharge (m^3/s)	Power (kVA)	Speed (r/min)			
116.2/124.9*	207	4.5	90.57/14.7	103.4*/0	150*	495/8.5		
T_m	T_w	T_d	T_n	b_p	b_t	T_y		
Time constants of governor starting-up (s)								
9	1.10	15	0.6	0.005	0.6	0.1		
R_a	R_b	R_r	R_i	R_o	L_p	L_r	c_b	c_r
Parameter value of rotor-bearing system (m)								
0.9	2.12	5	2.12036	2.185	0.587	2.5	0.36e−3	18e−3
I_f (A)	I (kA)	U_G(kV)	cos φ	U_L (KV)	Weight (t)	Rotor eccentricity (mm)		
Nominal/no-load value of excitor and generator								
1300/850*	4.32*/0	13.8*	0.885	12.21	955	0.7		

The '*' represent the basic value of the per unit

governor and generator and rotor-bearing models are listed in Table 1. The powerhouse model is built based on one actual project in China.

According to the subsystems introduced in Sect. 2, the whole system establishment of hydropower station is shown in Fig. 1, and the corresponding solution process is presented in Fig. 7. Firstly, the Ansys software is employed to set up the structures in this model, while others are dealt with by Fortran language. Then, the function of user-programmable features (UPFs) to compile Fortran program is used in order to facilitate the users that they can call these external commands anytime. In this way, the coupled hydraulic–mechanical–electric transient, in every time step, can be calculated for dynamic time history analysis, and the running process of unit can also be simulated. Thus, the study of dynamic characteristics for the coupled model of hydropower structure under different conditions can be achieved.

A simple description for computation process can be expressed as:

(1) Determine initial values of upstream boundary conditions H_1^n, Q_1^n and dynamic response of structure for this time step.
(2) Solve H_1^n and Q_1^n of each point in penstock model, by using the boundary conditions.
(3) Determine initial values for iteration n_{ep}, Q_{ep}, H_{enp}, τ_e. Solve P_t with characteristic curves and similarity law of water turbine.
(4) Determine E'_q from time last step. Solve P_e with the equations of the third-order generator model, the excitation regulation equation and the power grid equations.
(5) Solve speed n_p through Eq. (18), and judge whether the inequality $|n_p - n_{ep}|/n_s < 0.005$ is satisfied:
    (a) Yes, continue to step (6)
    (b) No, return to step (3) for calculation again with n_p, Q_p, H_{np} as iteration values.
(6) Solve τ with the help of governor model, and judge whether the inequality $|\tau - \tau_e| < 0.005$ is satisfied:
    (a) Yes, continue to step (7)
    (b) No, return to step (3) for calculation again with τ and the result from step (5), as iteration values.
(7) Calculate dynamic characteristics of guide bearing and the loads generated by hydraulic, mechanical and electric excitation sources. Solve and obtain the dynamic characteristics of the structures.
(8) Record the results and go to step (1) for next time step.

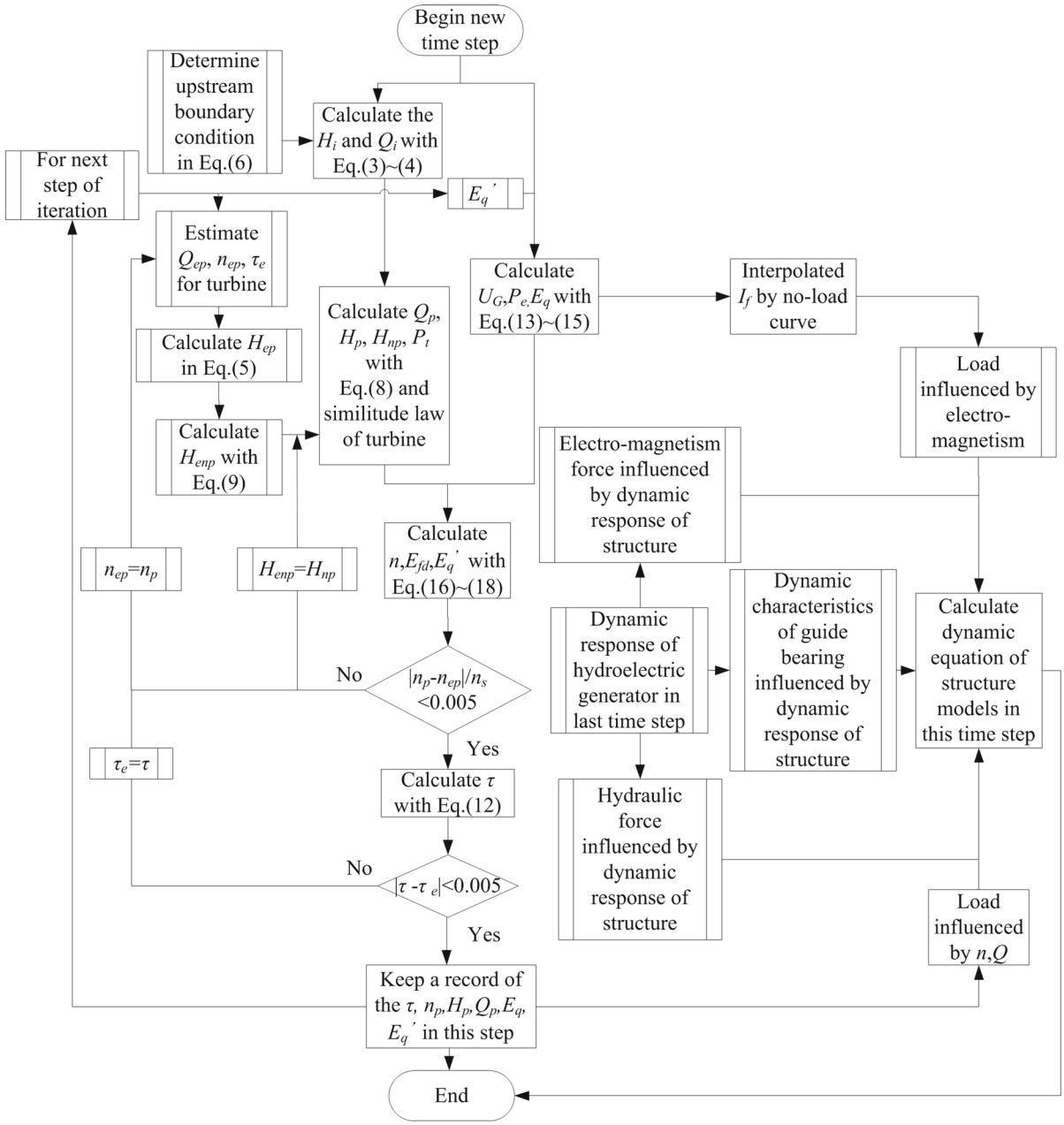

Fig. 7 Computational process of the system

4 Numerical calculation and result analysis

The variation properties of ω, τ and P_t from beginning to no load for the turbine are illustrated in Fig. 8. It can be seen that during the process of starting-up, ω rises smoothly with barely appearing overshoot phenomenon. The τ fast reaches the starting value in short time at first, then it begins to attenuate as ω increases to the rated point, and finally τ keeps stable with the constant no-load value. Meanwhile, in order to supply the motivation for accelerating rotating speed, the output power of turbine P_t also increases rapidly at the initial stage. When ω tends to be stable, P_t reduces to zero after experiencing a short variability process. The

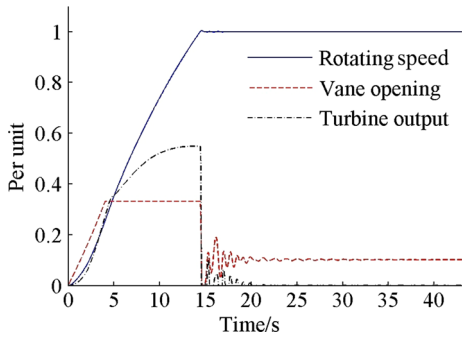

Fig. 8 Simulation result of starting-up transient

change laws as depicted in Fig. 8 are consistent with that in Reference [62].

Figure 9 shows the variation laws of discharge (Q) and head (H_n) for water turbine during the process from staring to no load. As depicted in Fig. 9a, Q has a fast increase at beginning, because of the quick enlargement for τ. When τ is stable with the starting value, Q begins to decrease smoothly. In the vicinity of $t = 15$ s, τ suddenly falls down to zero; correspondingly, the discharge of turbine turns to be none. Subsequently, Q starts to attenuate as the fluctuation of τ, and it becomes stable at $t = 22$ s. Similarly, the abrupt starting of guide vane leads to τ increase, while H_n experiences the process of decreasing at first, but increasing in the end, as shown in Fig. 9b. At $t = 15$ s, H_n soars until it reaches the peak value due to the sudden drop of τ (at this time, the great water pressure can be induced in penstock). After that, as the fluctuation of τ tends to be stable gradually, H_n follows the trend and becomes stable eventually. The change laws of Q and H_n follow the normal routine of water turbine during starting-up, namely they change with a wide range at beginning, then swing within a narrow range and turn to be stable finally.

Figures 10 and 11 present the diagram of displacements and trajectories for rotor and turbine, as well

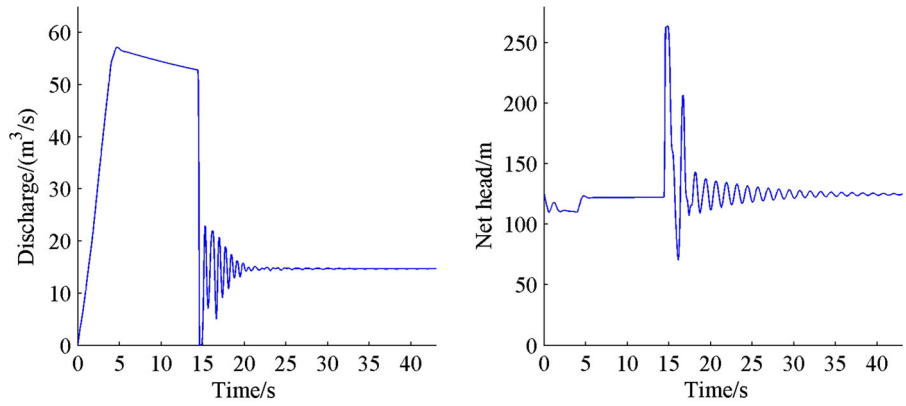

Fig. 9 Discharge and head change during starting-up

(a) Change of turbine discharge **(b)** Change of turbine net head

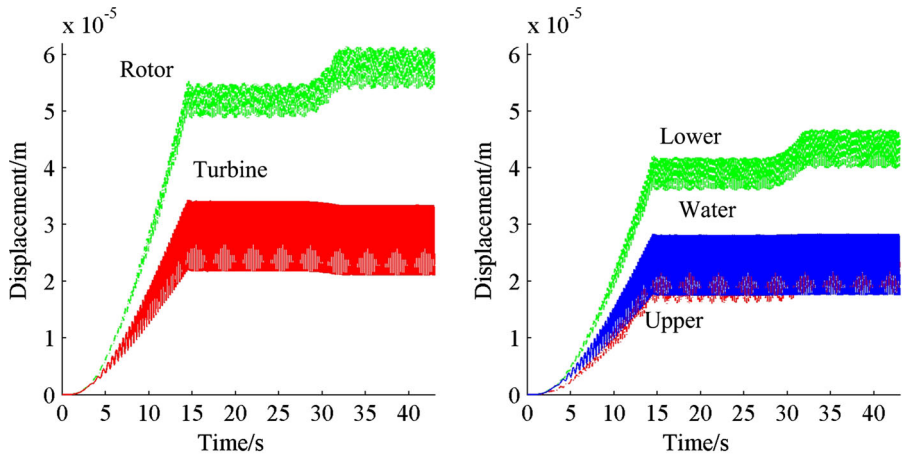

Fig. 10 Total axis displacement in horizontal direction

(a) Axis displacement of rotator **(b)** Axis displacement of guide bearings

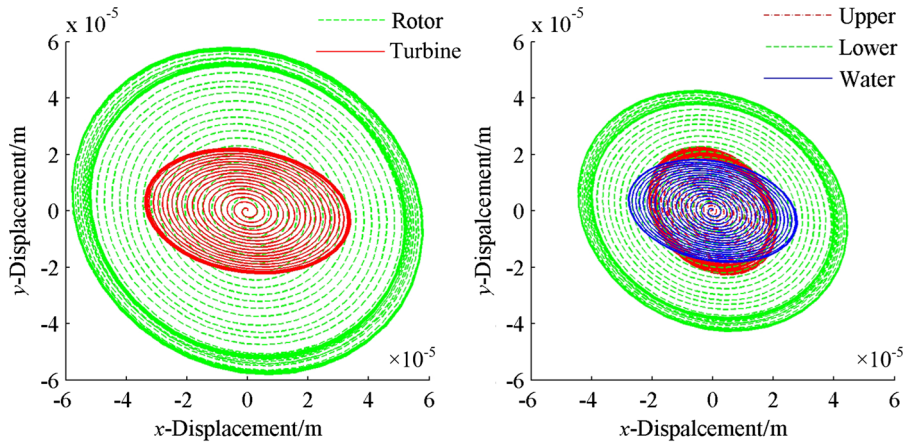

Fig. 11 Axis trajectories in horizontal direction

(a) Axis trajectories of rotator **(b)** Axis trajectories of guide bearings

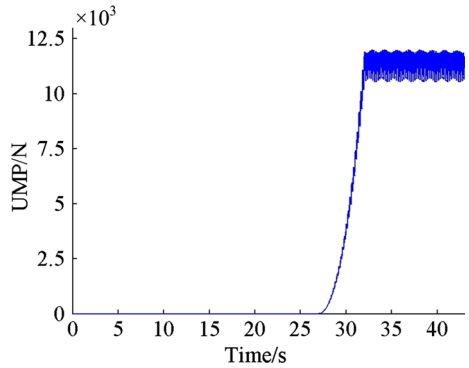

Fig. 12 Change of UMP during starting-up process

as guide bearings, respectively. Based on Fig. 10 with combination of the orbit in Fig. 11 and ω variation in Fig. 8, it can be known that before ω reaches rated value, the displacement of rotor, turbine and guide bearings always increases with increasing ω, and the displacement turns to be stable when ω equals rated point. For the rotor, due to the reason that it has a relatively great quality, accordingly, the eccentric force of rotor is larger than that of turbine; therefore, compared with turbine, the trajectory amplitude of rotor is larger, as shown in Fig. 10a. While the axis orbits of guide bearings in Fig. 10b are as similar as that in Fig. 10a, the descending order of amplitude for all guide bearings is lower bearing, water bearing and upper bearing, respectively, which reflects the effect of the vibration of rotor and turbine on every bearing, to some extent. In other words, the reason why the displacements of lower and water bearing are larger is that the distance between the lower bearing and rotor, as well as that between water bearing and turbine, is relatively close, making them to bear lager force from rotor and turbine, respectively.

In this paper, the building-up process of generator begins at $t = 27$ s during the starting-up process; at this time, the field current (I_f) appears synchronously and increases gradually; correspondingly, the UMP is produced and developed with the increase in I_f, as represented in Fig. 12. Combining Figs. 11 and 12, it can be observed that from $t = 27$ s, the amplitude for trajectory of rotor starts to be larger, while that of upper and lower bearing also increases to some degree. At $t = 32$ s, the UMP steps into stable period with small fluctuation, as shown in Fig. 12. On one hand, the phenomenon can be explained as that when terminal voltage reaches rated value, I_f is unchanged; accordingly, the UMP is also not varied. On the other hand, the value of UMP is influenced by dynamic response of rotor and may swing to a certain extent. In this case, the trajectories of rotor and lower bearing in Figs. 10 and 11 will arrive at a new stable stage, as UMP varies.

5 Conclusions

On the theoretical basis of hydraulics, electric machinery and structure etc., a whole model of the coupled hydro–mechanical–electric and structure for hydropower station system is established in this paper. With the help of UPFs function from Ansys software, the transient process analysis for the coupled system in every time step of the structural dynamic calculation is realized. The main conclusions are as follows:

(1) Multiple numerical methods are employed to simulate the variation laws of parameters during the starting process for one actual hydropower station in China. The results show good agreement with that from previous studies verifying the rationality of the model proposed in this paper.
(2) The change laws of eccentric forces and UMP in staring-up process are also simulated through numerical methods; meanwhile, the dynamic characteristics of shaft system under the two excitations are reflected, which further demonstrates the effectiveness of the model established in this paper.

It needs to be pointed out that there are several operation conditions such as starting-up, load up, load down and load rejection in the hydropower station system. However, only starting-up conditions are analyzed in this paper because of the limited space. Moreover, due to the reason that the water pressure fluctuation is small and the circle of stator winding is open during staring-up process, the pressure fluctuation and electromagnetic transient process are not considered. Nevertheless, the hydraulic and electric force belong to important excitation sources for hydropower station, whose existence will inevitably bring different influence on the operation conditions for hydropower station. In the future work, other operation conditions can be discussed, and the effect of these excitations on the system will be emphasized. In addition, the dynamic coupled relationship between pressure fluctuation and structural vibration characteristics can also be discussed. As a result, the relevant model can be improved to investigate the interlink ages, as well as dynamic characteristics among each submodule system for hydropower station under different conditions, in order to provide more sufficient theoretical basis for the safety operation of the system.

Acknowledgements This research is supported by the National Natural Science Foundation of China (No.51379030) and Youth Foundation of Taiyuan University of Technology (No. 2015QN029).

References

1. Chaudry, M.H.: Applied Hydraulic Transients. Springer, New York (2014)
2. Collatz, L.: The Numerical Treatment of Differential Equations. Springer, Berlin (1960)
3. Wylie, E.B., Streeter, V.L.: Fluid Transient in Systems. Prentice-Hall, Englewood Cliffs (1993)
4. Parmakian, J.: Water-Hammer Analysis. Prentice-Hall, Englewood Cliffs (1955)
5. Lighthill, J.: Waves in Fluids. Cambridge University Press, Oxford (1978)
6. Ghidaoui, M.S., Mansour, S.: Efficient treatment of the Vardy-Brown unsteady shear in pipe transients. J. Hydraul. Eng. ASCE **128**(1), 102–112 (2002)
7. Silva-Araya, W.F., Chaudhry, M.H.: Unsteady friction in rough pipes. J. Hydraul. Eng. ASCE **127**(7), 607–618 (2001)
8. Shuy, E.B.: Wall shear stress in accelerating and decelerating turbulent pipe flows. J. Hydraul. Res. **34**(2), 173–183 (1996)
9. Yang, J.C., Hsu, E.L.: On the use of the reach-back characteristics method of calculation of dispersion. Int. J. Numer. Methods Fluids **12**(3), 225–235 (1991)
10. Ruprecht, A., Helmrich, T.: Simulation of the water hammer in a hydro power plant caused by draft tube surge. In: 4th ASME/JSME Joint Fluids Engineering Conference. Honolulu (2003)
11. Panov, L.V., Chirkov, D.V., Cherny, S.G., et al.: Numerical simulation of pulsation processes in hydraulic turbine based on 3D model of cavitating flow. Thermophys. Aeromech. **21**(1), 31–43 (2014)
12. Zhang, X.X., Cheng, Y.G.: Simulation of hydraulic transients in hydropower systems using the 1-D-3-D coupling approach. J. Hydrodyn. Ser. B. **24**(4), 595–604 (2012)
13. Zhang, X.X., Cheng, Y.G., Yang, J.D., et al.: Simulation of the load rejection transient process of a Francis turbine by using a 1-D-3-D coupling approach. J. Hydrodyn. Ser. B. **26**(5), 715–724 (2014)
14. IEEE Committee, : Dynamic models for steam and hydro turbines in power system studies. IEEE Trans. Power Appar. Syst. **PAS-92**(6), 1904–1915 (1973)
15. Oldenburge, R., Donelson, J.: Dynamic response of a hydroelectric plant. Trans. Am. Inst. Electr. Eng. Part 3 **81**(3), 403–418 (1962)
16. Hovey, L.M.: Optimum adjustment of hydro governors on Manitoba hydro system. Trans. Am. Inst. Electr. Eng. Part 3 **81**(3), 581–586 (1962)
17. Sanathanan, C.K.: Accurate low order model for hydraulic turbine-penstock. IEEE Trans. Energy Convers. **EC–2**(2), 196–200 (1987)
18. Vournas, C.D.: Second order hydraulic turbine models for multimachine stability studies. IEEE Trans. Energy Convers. **5**(2), 239–244 (1990)
19. Paynter, H.M.: A Palimpsest on the Electronic Analog Art. A. Philbrick Researches Inc., Boston (1955)
20. Leum, M.: The development and field experience of a transistor electric governor for hydro turbines. IEEE Trans. Power Appar. Syst. **PAS–85**(4), 393–402 (1966)
21. Phi, D.T., Bourque, E.J., Thorne, D.H., et al.: Analysis and application of the stability limits of a hydro-generating unit. IEEE Trans. Power Appar. Syst. **PAS–100**(7), 3203–3212 (1981)
22. Hagihara, S., Yokota, H., Goda, K., et al.: Stability of a hydraulic turbine-generating unit controlled by PID governor. IEEE Trans. Power Appar. Syst. **PAS–98**(6), 2294–2298 (1979)
23. Murphy, L.D., Wozniak, L., Whittemore, T.A.: A digital governor for hydro generators. IEEE Trans. Energy Convers. **3**(4), 780–784 (1989)

24. Anwar, M.N., Pan, S.: A new PID load frequency controller design method in frequency domain through direct synthesis approach. Int. J. Electr. Power Energy Syst. **67**, 560–569 (2015)
25. Kamwa, I., Lefebvre, D., Loud, L.: Small Signal Analysis of Hydro-Turbine Governors in Large Interconnected Power Plants. IEEE Power Engineering Society Winter Meeting, New York (2002)
26. Wozniak, L., Filbert, T.L.: Speed loop cancellation governor for hydrogenerators—part I: development. IEEE Trans. Energy Convers. **3**(1), 85–90 (1988)
27. Li, H., Chen, D., Zhang, H., et al.: Nonlinear modeling and dynamic analysis of a hydro-turbine governing system in the process of sudden load increase transient. Mech. Syst. Signal Process. **80**, 414–428 (2016)
28. Zhang, H., Chen, D., Xu, B., et al.: Nonlinear modeling and dynamic analysis of hydro-turbine governing system in the process of load rejection transient. Energy Convers. Manag. **90**, 128–137 (2015)
29. Xu, B., Wang, F., Chen, D., et al.: Hamiltonian modeling of multi-hydro-turbine governing systems with sharing common penstock and dynamic analyses under shock load. Energy Convers. Manag. **108**, 478–487 (2016)
30. Kilgore, L.A.: Calculation of synchronous machine constants-reactances and time constants affecting transient characteristics. Trans. Am. Inst. Electr. Eng. **50**(4), 1201–1213 (1931)
31. Wright, S.H.: Determination of synchronous machine constants by test reactances, resistances and time constants. Trans. Am. Inst. Electr. Eng. **50**(4), 1331–1350 (1931)
32. Heffron, W.G., Phillips, R.A.: Effect of a modern amplidyne voltage regulator on underexcited operation of large turbine generators. IEEE Trans. Power Appar. Syst. **71**(1), 692–697 (1952)
33. Sayidi, A.M., Nekoui, M.A., Boghrabidi, N.S.: Adaptive optimal control for a one-machine infinite-bus power system. In: International Conference on Computational Intelligence for Modeling Control and Automation, Vienna (2008)
34. Demello, F.P., Laskowski, T.F.: Concepts of power system dynamic stability. IEEE Trans. Power Appar. Syst. **PAS–94**(3), 827–833 (1975)
35. Demello, F.P., Concordia, C.: Concepts of synchronous machine stability as affected by excitation control. IEEE Trans. Power Appar. Syst. **PAS–88**(4), 316–329 (1969)
36. Zhong, Y.E., He, Y.Z., Wang, Z., et al.: Rotor Dynamics. Tsinghua University Press, Beijing (1987)
37. Wen, B.C., Gu, J.L., Xia, S.B., et al.: Senior Rotor Dynamics. China Machine Press, Beijing (2000)
38. Earles, L.L., Palazzolo, A.B., Armentrout, R.W.: A finite element approach to pad flexibility effects in tilt pad journal bearings: part 1—single pad analysis. J. Tribol. **112**(2), 178–182 (1990)
39. Ma, Z.Y., Dong, Y.X.: Dynamic coefficients of tilting pad guide bearings of hydraulic turbine set. Power Eng. **10**(6), 6–11 (1990)
40. Adiletta, G., Guido, A.R., Rossi, C.: Nonlinear dynamics of a rigid unbalanced rotor in journal bearings. Part I: theoretical analysis. Nonlinear Dyn. **14**(1), 57–87 (1997)
41. Adiletta, G., Guido, A.R., Rossi, C.: Nonlinear dynamics of a rigid unbalanced rotor in journal bearings. Part II: Experimental analysis. Nonlinear Dyn. **14**(2), 157–189 (1997)
42. Rho, B.H., Kim, K.W.: A study of the dynamic characteristics of synchronously controlled hydrodynamic journal bearings. Tribol. Int. **35**(5), 339–345 (2002)
43. Tiwari, R., Lees, A.W., Friswell, M.I.: Identification of speed-dependent bearing parameters. J. Sound Vib. **254**(5), 967–986 (2002)
44. Xu, Y., Li, Z.H., Lai, X.D.: Dynamic model for hydroturbine generator units based on a database method for guide bearings. Shock Vib. **20**(3), 411–421 (2013)
45. Zhang, L.K., Ma, Z.Y., Song, B.W.: Dynamic characteristics of a rub-impact rotor-bearing system for hydraulic generating set under unbalanced magnetic pull. Arch. Appl. Mech. **83**(6), 817–830 (2013)
46. Zeng, Y., Zhang, L.X., Guo, Y.K., et al.: The generalized Hamiltonian model for the shafting transient analysis of the hydro turbine generating sets. Nonlinear Dyn. **76**(4), 1921–1933 (2014)
47. Xu, B.B., Chen, D.Y., Zhang, H., et al.: Dynamic analysis and modeling of a novel fractional-order hydro-turbine-generator unit. Nonlinear Dyn. **81**(3), 1263–1274 (2015)
48. Gustavsson, R.K., Aidanpää, J.O.: Evaluation of impact dynamics and contact forces in a hydropower rotor due to variations in damping and lateral fluid forces. Int. J. Mech. Sci. **51**(9–10), 653–661 (2009)
49. Zhang, L.K., Ma, Z.Y., Wu, Q.Q., et al.: Vibration analysis of coupled bending-torsional rotor-bearing system for hydraulic generating set with rub-impact under electromagnetic excitation. Arch. Appl. Mech. (2016). doi:10.1007/s00419-016-1142-8
50. Xu, W., Ma, Z.Y., Zhi, B.P.: Analysis on power flow transmission of pressure fluctuation along the walls of hydropower house. J. Hydroelectr. Eng. **32**(2), 233–239 (2013)
51. Zhang, Y.L., Ma, Z.Y., Chen, G.R., et al.: Strength and stiffness analysis of spiral casing with different embedded manners. J. Hydraul. Eng. **37**(10), 1206–1211 (2006)
52. Zhang, C.H., Ma, Z.Y., Zhou, S.D., et al.: Analysis of fluid–solid interaction vibration characteristics of large-scale hydropower house. J. Hydroelectr. Eng. **31**(6), 192–197 (2012)
53. Sun, W.Q., Huang, X.H.: Identification of vibration transfer path for the coupled system of water turbine generator set and power house. J. Vib. Shock. **33**(6), 23–28 (2014)
54. Song, Z.Q.: Research on Coupling Vibration Characteristics of Generator Set and Hydropower House. Dalian University of Technology, Dalian (2009)
55. Yang, X.M.: Research on Generating Set Vibration and Coupled that and Hydropower House Vibration in Hydropower Station. Dalian University of Technology, Dalian (2006)
56. Chen, Z., Chen, S.S., Zhang, Z.H., et al.: Effect of hydraulic system models on power system transient stability analysis. J. Tsinghua Univ. Sci. Technol. **36**(7), 13–18 (1996)
57. Chen, Z., Diao, Q.H., Chen, S.S., et al.: Study on the effect of hydraulic system models on power system dynamic stability analysis. J. Tsinghua Univ. Sci. Technol. **36**(7), 69–74 (1996)
58. Zhao, G.L.: Study on the United Transient Process for Hydraulic Mechanical and Power System. Wuhan University, Wuhan (2004)
59. Guo, W.C., Yang, J.D., Yang, W.J., et al.: Regulation quality for frequency response of turbine regulating system of

isolated hydroelectric power plant with surge tank. Int. J. Electr. Power Energy Syst. **73**, 528–538 (2015)
60. Fang, H.Q., Chen, L., Dlakavu, N., et al.: Basic modeling and simulation tool for analysis of hydraulic transients in hydroelectric power plants. IEEE Trans. Energy Convers. **23**(3), 834–841 (2008)
61. Committee, I.E.E.E.: Hydraulic-turbine and turbine control-models for system dynamic studies. IEEE Trans. Power Syst. **7**(1), 167–179 (1992)
62. Bao, H.Y., Yang, J.D., Fu, L.: Study on nonlinear dynamical model and control strategy of transient process in hydropower station with Francis turbine. In: Asia-Pacific Power and Energy Engineering Conference, Wuhan (2009)